Metrol. Meas. Syst., Vol. 30 (2023), No. 1
DOI: 10.24425/mms.2023.144398

METROLOGY AND MEASUREMENT SYSTEMS
Index 330930, ISSN 0860-8229
www.metrology.wat.edu.pl

DYNAMIC TILT TESTING OF MEMS INCLINOMETERS BASED ON CONICAL MOTIONS

Qihang Yang[1)], Chenguang Cai[2)], Ming Yang[3)], Ming Kong[1)], Zhihua Liu[2)], Feng Liang[4)]

1) *College of Metrology and Measurement Engineering, China Jiliang University, Hangzhou 310018, China* (*boon617@163.com, mkong@cjlu.edu.cn*)
2) *National Institute of Metrology of China, Beijing 100013, China* (*caichenguang@nim.ac.cn*, ✉ *liuzhihua@nim.ac.cn*)
3) *College of Electrical Engineering, Guizhou University, Guiyang 550025, China* (*myang23@gzu.edu.cn*)
4) *Shenyang Aircraft Corporation, Shenyang 110031, China* (*304803532@qq.com*)

Abstract

The MEMS inclinometer integrates a tri-axis accelerometer and a tri-axis gyroscope to solve the perceived dynamic inclinations through a complex data fusion algorithm, which has been widely used in the fields of industrial, aerospace, and monitoring. In order to ensure the validity of the measurement results of MEMS inclinometers, it is necessary to determine their dynamic performance parameters. This study proposes a conical motion-based MEMS inclinometer dynamic testing method, and the motion includes the classical conical motion, the attitude conical motion, and the dual-frequency conical motion. Both the frequency response and drift angle of MEMS inclinometers can be determined. Experimental results show that the conical motions can accelerate the angle drift of MEMS inclinometers, which makes them suitable for dynamic testing of MEMS inclinometers. Additionally, the tilt sensitivity deviation of the MEMS inclinometer by the proposed method and the turntable-based method is less than 0.26 dB. We further provide the research for angle drift and provide discussion.

Keywords: MEMS inclinometer, sensitivity, dynamic testing, conical motion, angle drift.

1. Introduction

Because MEMS inclinometers have the advantages of small size, low cost, and high performance, they are widely used in structural health monitoring, ground motion detection, aerospace, industrial control, and other application fields [1-4]. The MEMS inclinometer is composed of a tri-axis gyroscope and a tri-axis accelerometer. The gyroscope can measure the angular velocity of a dynamic object and calculate dynamic angles through integration of the measured angular velocity with high accuracy in a short time [5, 6]. At the same time the accelerometer can obtain the high-precision tilt angle of a static object [7-9] from the acceleration measurement with reference to gravity. Depending on the complementarity of the internal gyroscope and accelerometer, the MEMS inclinometer system obtains the inclination measurement through a complex data fusion algorithm. The measurement results of MEMS inclinometers require thorough dynamic testing.

Most existing testing methods use the static position method and dynamic rate method [10-12] to calibrate the error model of the MEMS accelerometer and the MEMS gyroscope inside [13, 14]. Xu *et al.* [15] specifically studied the scale factor of the MEMS accelerometer and obtained the scale factor testing results for three positions by gravity or single acceleration. Särkkä *et al.* [16, 17] established mathematical models for sensor parameters such as zero bias, scale factor, and cross coupling error, and then carried out static tests on sensors in multiple positions through the improved multi-position testing method. These static testing methods do

Article history: received July 17, 2022; revised September 19, 2022; accepted September 26, 2022; available online January 23, 2023.

not to some extent rely on precision turntables but require a highly accurate mounting frame so that the position of the sensitive axis of the accelerometer coincides with the reference frame as closely as possible. The dynamic rate testing method usually requires a precision rate turntable or angular shaking table to rotate or vibrate at a given rate. Then the output of the gyroscope is compared with that of the platform to evaluate the performance of the gyroscope. Shang *et al.* [18, 19] used the cosine signal of a single-axis turntable as a continuous excitation signal to obtain those parameters in the mathematical model of the gyroscope by comparing the input and output of the gyroscope. Although the testing method is simple, it still requires high precision from the turntable and a high precision installation rack. Some scholars proposed mounting the gyroscope on the rotary table with a square frame. Adopting the static north finding method [20] and performing alignment operations in four positions, its posture information can be used for horizontal posture initialization. This method can achieve long-term attitude holding. However, it requires building a complex parameter model. Also, it is not convenient for attitude tracking. Other researchers used multi-axis turntables or centrifuge equipment, but these testing methods were much more dependent on the accuracy of the equipment [21-24]. Cheng *et al.* [25] proposed establishing a gyroscope calibration model according to the relationship between the output of the accelerometer and the output of the gyroscope. This method does not require additional reference, but the accuracy of calibration is affected by the accuracy of the accelerometer.

Dynamic testing of the data fusion algorithm remains to be studied. The conical motion can provide two axial inclination changes, which has an advantage in tilt testing [26]. For inertial tilt measurement, conical motion is a poor working condition, which will not only introduce non-commutative error influence but also more easily induce the angle drift of algorithm calculations [27, 28].

In this study, dynamic tilt testing of MEMS inclinometers based on conical motion is investigated, which is organized as follows: Section 2 introduces three kinds of mathematical models of the conical motion; Section 3 elaborates on the synthesis method of the conical motion on the 6-DOF Stewart platform; in Section 4, the internal algorithm of MEMS inclinometers is tested by the generated conical motion. The frequency response and the angle drift of MEMS inclinometers are analyzed; the last section gives the conclusions.

2. Mathematical principles of the conical motion

Classical conical motion is a common method for dynamic testing of MEMS inclinometers. In fact, it is an ideal mode of the conical motion. It assumes that the body coordinate system coincides with the reference coordinate system completely and that there exist angular oscillations of the same frequency on the two orthogonal axes. Due to the influence of the changing external environment and control errors introduced by the driver [29], attitude conical motion or dual-frequency conical motion may also occur [30]. The attitude conical motion is generated when the two reference frames do not coincide completely because of the installation error. The attitude conical motion takes the deflection of the coordinate system into account and simulates a more practical working state of the environment. The dual-frequency conical motion is considered under more extreme conditions induced by the driver's control error. It is generated when the angular vibration frequencies of two orthogonal axes are different, which contains more pose information and is more conducive to dynamic tilt testing of MEMS inclinometers. Mathematical models of these three conical motions will be established in the following subsections.

2.1. Classical conical motion

As shown in Fig. 1, the classical conical motion around the Z-axis is described by the X- and Y- axes vibrating at the same frequency but with different phase angles, and the Z-axis moves conically around its equilibrium position in space. It is assumed that the *Oz* axis overlaps the conical surface with half conical angle α, and the *Ox* axis and *Oy* axis swing slightly around the equilibrium positions *Ox* and *Oy*, respectively. *OL* is a ray in the *XOY* plane.

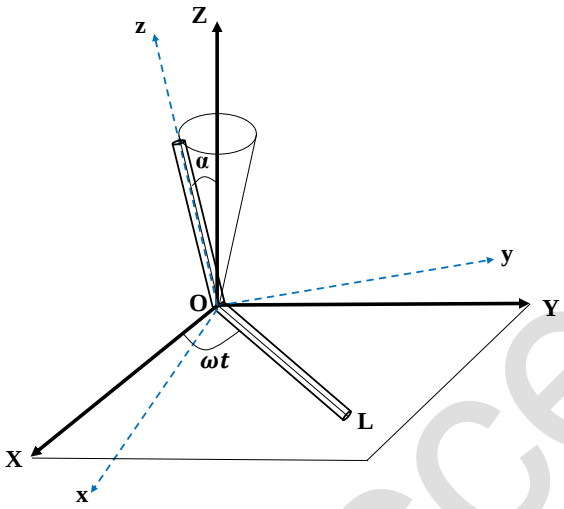

Fig. 1. Classical conical motion around the Z-axis.

Referring to Euler's rotation theorem, the *O-XYZ* coordinate system (*R*-system) is transformed to the *O-xyz* coordinate system (*B*-system), which is equivalent to the *R* system rotating α angle around the *OL* axis. Assume that the unit vector in the *OL* direction is

$$u_L(t) = [\cos\omega t \quad \sin\omega t \quad 0]' \tag{1}$$

The coordinate transformation matrix from the *R*-system to the *B*-system is

$$C_R^B = E + 2R\sin\frac{\alpha}{2}\cos\frac{\alpha}{2} + (1-\cos\alpha)R\times R \tag{2}$$

$$R = \begin{bmatrix} 0 & 0 & \sin\omega t \\ 0 & 0 & -\cos\omega t \\ -\sin\omega t & \cos\omega t & 0 \end{bmatrix}, \tag{3}$$

where *E* stands for the identity matrix, and the conical motion quaternion $q(t)$ rotating about the *Z*-axis is constructed.

$$q(t) = \begin{bmatrix} q_0 & q_1 & q_2 & q_3 \end{bmatrix}' = \begin{bmatrix} \cos\frac{\alpha}{2} & \sin\frac{\alpha}{2}\cos\omega t & \sin\frac{\alpha}{2}\sin\omega t & 0 \end{bmatrix}' \tag{4}$$

According to (2) (3) and (4), the coordinate transformation matrix can be expressed in terms of the quaternion as

$$C_R^B = \begin{bmatrix} q_0^2+q_1^2-q_2^2-q_3^2 & 2(q_1q_2-q_0q_3) & 2(q_1q_3+q_0q_2) \\ 2(q_1q_2+q_0q_3) & q_0^2-q_1^2+q_2^2-q_3^2 & 2(q_2q_3-q_0q_1) \\ 2(q_1q_3-q_0q_2) & 2(q_2q_3+q_0q_1) & q_0^2-q_1^2-q_2^2+q_3^2 \end{bmatrix} \tag{5}$$

2.2. Attitude conical motion

The body coordinate system (*T*-system) and the reference coordinate system (*R*-system) cannot completely coincide in actual installation, as shown in Fig. 2. When *T*-system $O\text{-}x_t y_t z_t$ has small attitude angles φ, θ and γ relative to *R*-system $O\text{-}x_r y_r z_r$, angular vibration exists in all three axes of *T*-system. Nevertheless, it can still be regarded as classical conical motion in the *R*-system. Therefore, the attitude conical motion is also called the classical conical motion along the reference coordinate system.

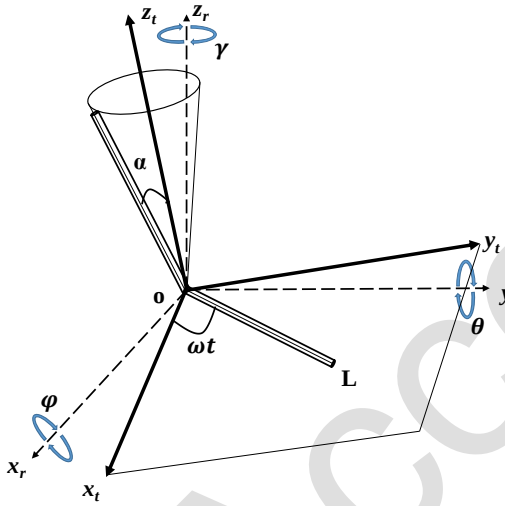

Fig. 2. Attitude conical motion around the Z-axis.

In the *T*-system, the influence of attitude angle deflection should be considered. The rotation matrix of the attitude angle is given by (6), where c=cos, s=sin.

$$R_q = \begin{bmatrix} c\theta c\gamma & s\varphi s\theta c\gamma - c\varphi s\gamma & s\varphi s\gamma + c\varphi s\theta c\gamma \\ c\theta s\gamma & s\varphi s\theta s\gamma + c\varphi c\gamma & c\varphi s\theta s\gamma - s\varphi c\gamma \\ -s\theta & s\varphi c\theta & c\varphi c\theta \end{bmatrix} \tag{6}$$

In the *R*-system, the quaternion $q(t)$ and its corresponding rotation matrix are the same as in (4) and (5), and the resultant rotation matrix obtained in the *T*-system is shown in (7).

$$C_T = R_q \cdot C_R^B \tag{7}$$

2.3. Dual-frequency conical motion

The dual-frequency conical motion vibrates with different frequencies in two orthogonal axes, as shown in Fig. 3. The motion generated in space with an angular vibration frequency ω_1 of the *X*-axis and ω_2 of the *Y*-axis not a simple conical motion but a relatively complex space periodic motion.

The rotation vector in the body coordinate system is given by

$$\Phi = \begin{bmatrix} \Phi_x & \Phi_y & \Phi_z \end{bmatrix}' = \begin{bmatrix} \alpha\cos\omega_1 t & \alpha\sin\omega_2 t & 0 \end{bmatrix}'. \tag{8}$$

The corresponding conical quaternion expression is constructed as (9). By substituting the quaternion of (9) into the coordinate transformation matrix of (5), the coordinate transformation matrix expression of the dual-frequency conical motion is modelled. This type of conical motion degrades to the classical conical motion as the two vibration frequencies ω_1 and ω_2 are equal.

$$q(t) = [\sqrt{1-(\sin\frac{\alpha}{2})^2 * ((\cos\omega_1 t)^2 + (\cos\omega_2 t)^2)} \quad \sin\frac{\alpha}{2}\cos\omega_1 t \quad \sin\frac{\alpha}{2}\sin\omega_2 t \quad 0]' \tag{9}$$

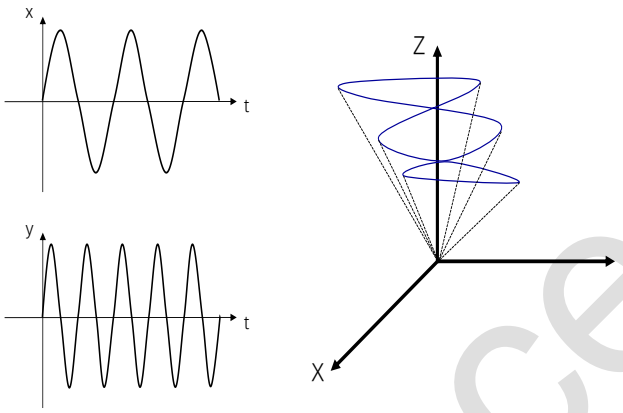

Fig. 3. Dual-frequency conical motion around the Z-axis.

3. Synthesis of the conical motion

The 6-DOF Stewart platform is used to generate the conical motion because of the following advantages it has. Firstly, it can get arbitrary pose motion in the workspace, and it has the benefit of generating the conical motion which provides angle variation of two degrees of freedom. Secondly, compared with the trajectory generated by the multi-axis turntable, the tip of the conical motion formed by the Stewart platform is not fixed. The position of the tip can be changed by parameter setting, providing higher flexibility for the testing of MEMS inclinometers.

Kinematics is used for controlling and measuring the Stewart platform, as shown in Fig. 4. We make (***t***,***q***) stand for the position and orientation of the Stewart platform. Inverse kinematics is implemented for calculating the length value of legs ***L*** of the Stewart platform. And the actual values ***L***', generated after adjusting by the servo motor, are used to get more accurate motion of the position and orientation by utilizing the forward kinematics program. The actual motion from the moving platform of the Stewart platform can be used for further testing [26].

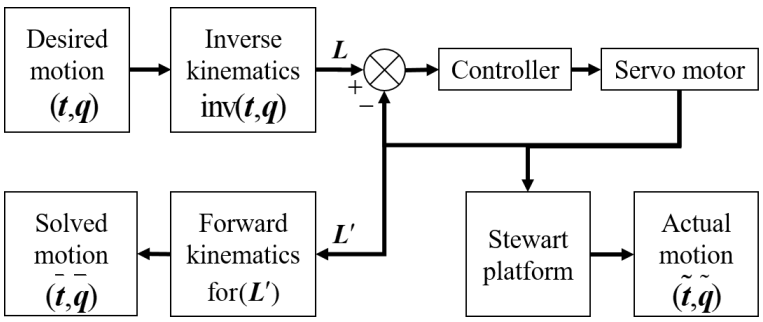

Fig. 4. Controlling and measuring of the position and orientation of the Stewart platform.

The control system for the conical motion from the 6-DOF Stewart platform is shown in Fig. 5. The motion program determines the dynamic conical quaternion and calls the inverse kinematics program, which calculates the command length values of the branch chain for the Stewart platform after each call. The host computer obtains the actual length values of the branch chain by reading the value of the inner encoder. The servo motor is operated independently through a three closed-loop control. Adjusting by PID from position-loop, speed-loop, and current-loop, the servo motor feeds the command back to the controller.

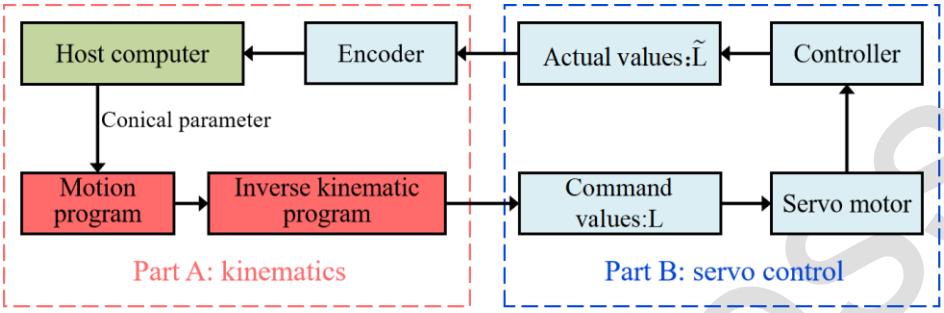

Fig. 5. Control system of the Stewart platform.

The flow chart of the synthesis of the conical motion is shown in Fig. 6. It is necessary to select the motion plane used to generate the spatial cone and set the conical parameters such as motion frequency, amplitude, and conical point coordinates into the motion program. Then the conical quaternion with attitude information is programmed in the motion program, and the cyclic controlled dynamic conical quaternion $q(t)$ is formed through time accumulation. We set the coordinate system in the segmentation mode and the trajectory is created by computing intermediate segment points with a coarse interpolation algorithm in milliseconds. Then, we put the motion program in the uniform cubic spline mode so as to execute a fine interpolation using a cubic spline algorithm every servo cycle. The motion program communicates with the inverse kinematic program in real time, converts the quaternion to the coordinate transformation matrix, and calculates the expansion and contraction of the branch chain of the 6-DOF Stewart platform under different conical poses.

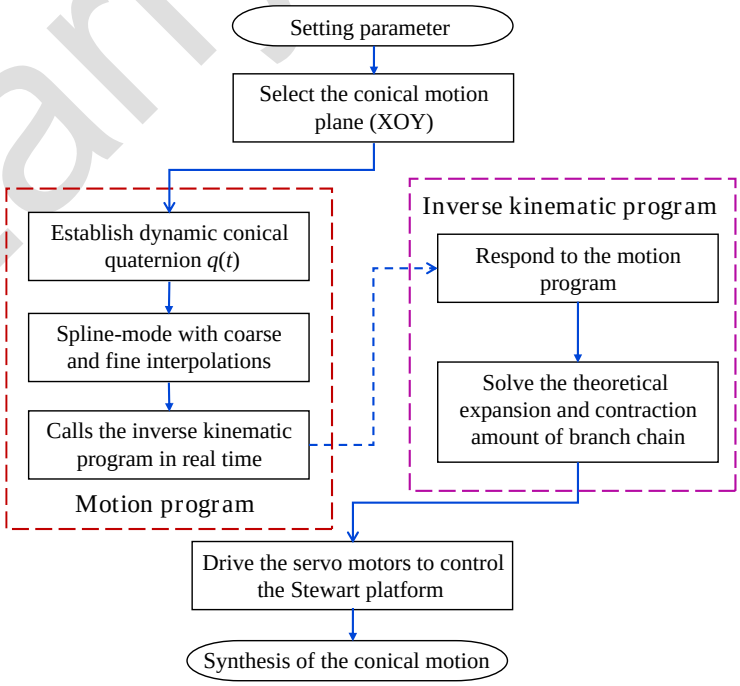

Fig. 6. Flow chart of the synthesis of the conical motion.

The quaternion representation method is more advantageous in the motion program. Compared with the Euler angle representation method, it neglects to consider the effect of rotation order during coordinate transformation, which improves the transformation efficiency of the rotation matrix. In addition, in order to obtain a more accurate expansion and contraction amount of the branch chain, we add rough interpolation and fine interpolation into the motion program and inverse kinematic program severally.

4. Experimental research

The dynamic testing system composed of the Stewart platform is shown in Fig. 7. The MEMS inclinometer under test is installed on the moving platform so that the horizontal roll-axis and vertical pitch-axis are parallel to the *X*-and *Y*-axes of the 6-DOF Stewart platform.

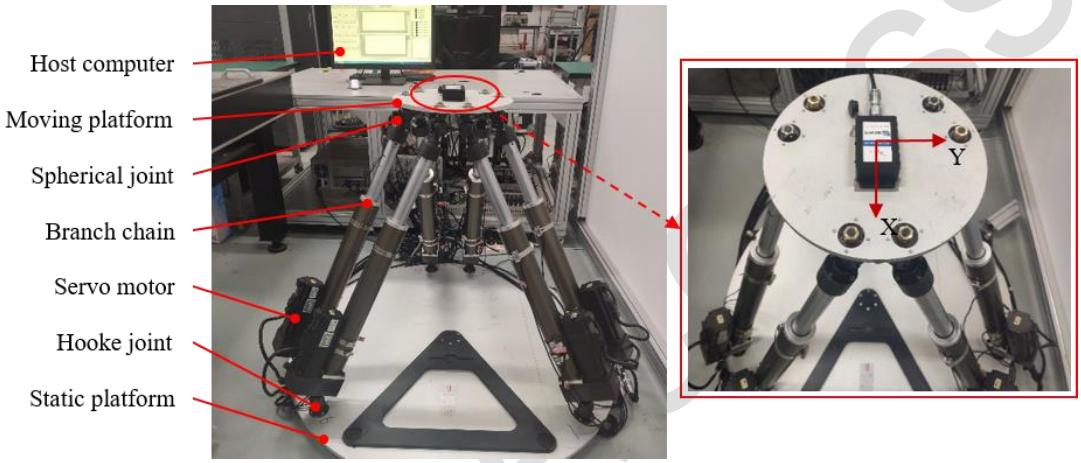

Fig. 7. Testing system for MEMS inclinometers.

The 6-DOF Stewart platform is controlled to generate the specific conical motion. The sensed tilt of the MEMS inclinometer is recorded. Meanwhile, the leg lengths of the 6-DOF Stewart platform are uploaded to the host computer. The six branch chains are collected by the host computer, and the 6-DOF Stewart platform pose is solved by forward kinematics. Due to the influence of closed-loop frequency response characteristics, amplitude attenuation and phase delay in the servo control system, there result errors between the actual and the command leg lengths. Therefore, the actual pose of the 6-DOF Stewart platform is obtained by solving the forward kinematics from the measured leg lengths. The sensitivity of tilt amplitude and the influence of data drift can be determined by comparing the inclination data of the MEMS inclinometer with that of the Stewart platform.

A BW-VG500 was used in the experiment whose parameters are shown in Table 1.

Table 1. Performance parameters of the tested MEMS inclinometer.

Model	BW-VG500
Attitude parameter	Dynamic precision: 0.1°
Compensation characteristics	Nonlinear compensation
	Quadrature compensation
	Gyro drift compensation
Internal algorithm	Kalman filter algorithm

4.1. Testing results for the classical conical motion

The 6-DOF Stewart platform generates the classical conical motion by rotating around the *Z*-axis. Testing points are selected ranging from 0.1 Hz to 4 Hz. Two frequencies, 0.1Hz and 4Hz, were selected for repeatability tests using the Bessel formula and we list the solved standard deviation values in Table 2. Experiments show that the repeatability of both the MEMS inclinometer and the 6-DOF Stewart platform performs well. However, the used 6-DOF Stewart platform does not meet the requirements when frequency exceeds 4Hz, so we. Thus, we only verify experimental data within 4Hz as the highest frequency of rotation. The data in the following experiments is averaged over five replicates.

Table 2. Calculated standard deviation values for the MEMS inclinometer and the 6-DOF Stewart platform.

Frequency (Hz)	MEMS inclinometer		6-DOF Stewart platform	
	Roll	Pitch	X	Y
0.1	9.02E-04	5.00 E-04	1.39E-05	1.95E-05
4	2.45 E-04	3.24 E-04	9.90E-05	8.87E-05

Within the capabilities of platform performance, the conical angle is set to 10° at low frequencies and gradually decreases with the increase of frequency. The tilt sensitivity defined in (10) was used to reflect the performance characteristic of the MEMS inclinometer.

$$S = 20 * \lg \frac{A_1}{D}, \tag{10}$$

where A_1 is stands for the collected tilt angle of the MEMS inclinometer and D is the actual motion inclination angle of the conical motion generated by the 6-DOF Stewart platform.

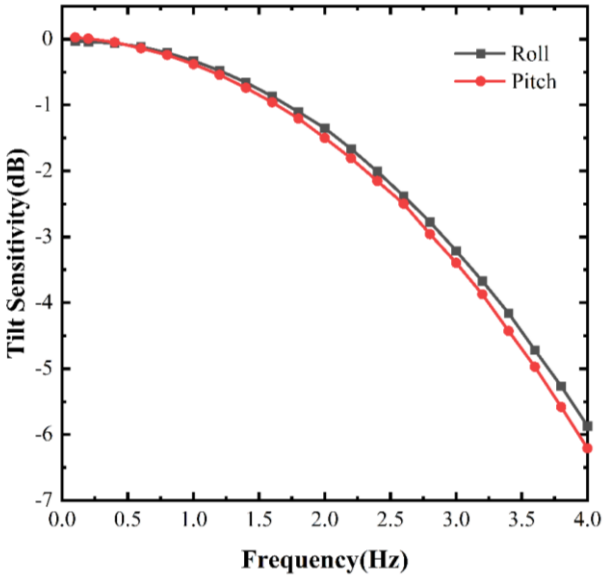

Fig. 8. Performance characteristic curve of the MEMS inclinometer in classical conical motion test.

Figure 8 shows the performance characteristic curve of the MEMS inclinometer under the classical conical motion. When the motion frequency is within the limits of 0.1 Hz to 0.6 Hz, the axial output inclination of the MEMS inclinometer is basically consistent with the actual motion angle of the platform, and the dynamic performance of the MEMS inclinometer is relatively stable. The tilt sensitivity of the MEMS inclinometer fades as the frequency exceeds

0.6 Hz, and the attenuation rate increases gradually. At 3.4 Hz, the tilt sensitivity attenuation of the MEMS inclinometer exceeds 4 dB, and the sensitivity of tilt degree is less than 63%, indicating poor dynamic tracking performance of the sensor. When the motion frequency reaches 4 Hz, the amplitude sensitivity of the MEMS inclinometer falls to 6 dB, and the perception degree of inclination is only 50%, which makes it difficult to meet the needs of most dynamic measurement applications.

The effectiveness of the testing method based on conical motions is verified by the comparative experiment of the turntable. We installed the MEMS inclinometer on the table of the turntable and adjusted the sensitive axis of the sensor to be parallel to the movement direction of the turntable, as shown in Fig. 9. In order to reduce the error of repeated installation, the sensitive axis for another group of experiments can be adjusted to be parallel to the outer axis of the turntable by rotating the inner axis of the two-axis turntable. The outputs of the MEMS inclinometer under different amplitude-frequency conditions are tested by using the one-dimensional sinusoidal swing motion generated by the two-axis precision turntable so as to obtain the tilt sensitivity of the MEMS inclinometer.

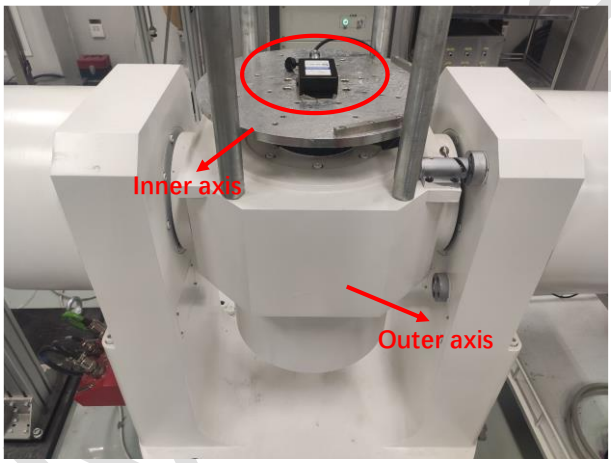

Fig. 9. Installation for the two-axis turntable test.

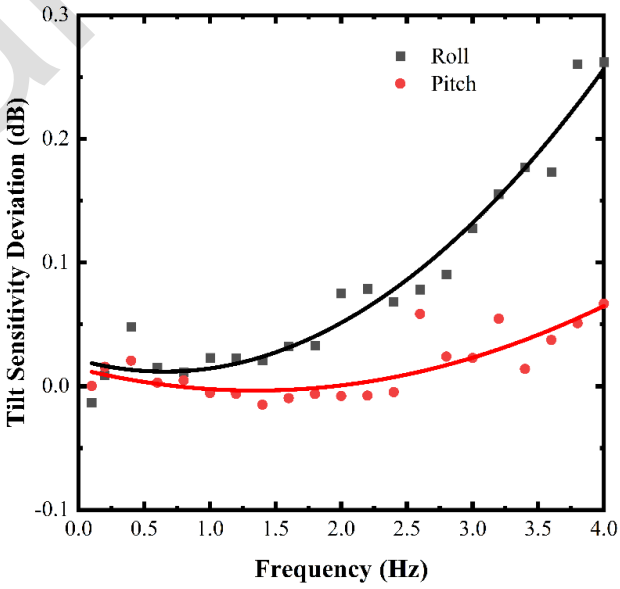

Fig. 10. Tilt sensitivity deviation of the MEMS inclinometer in the two-platform test.

From the conical motion results and the turntable angle data, we obtain the difference in testing values of the MEMS inclinometer sensitivity. As shown in Fig. 10 and Table 3, the maximum deviation is less than 0.26 dB. The angle output results from the classical conical motion generated by the 6-DOF Stewart platform match well with those of the precision turntable.

Table 3. Partial data for tilt sensitivity deviation.

	Frequency (Hz)								
	0.1	0.6	1	1.6	2	2.6	3	3.6	4
Roll-axis	-0.0130	0.0154	0.0231	0.0321	0.0750	0.0782	0.1277	0.1733	0.2596
Pitch-axis	0.0002	0.0029	-0.0055	-0.010	-0.0080	0.0585	0.0229	0.0375	0.0670

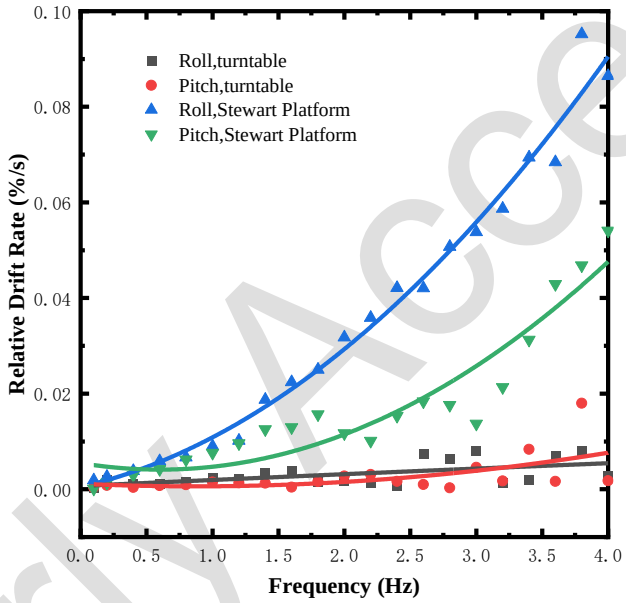

Fig. 11. Drift trend diagram of the MEMS inclinometer in the two-platform test.

The internal gyroscope of the MEMS inclinometer can obtain inclination data indirectly by integrating angular velocity, and the integral operation will inevitably lead to data drift. The conical motion test measurement data were analysed, and the relative drift rate V_p of the MEMS inclinometer was calculated using (11).

$$V_p = \frac{V_1}{D}, \tag{11}$$

where V_1 is the inclination drift rate output of the MEMS inclinometer, and the definition of D is the same as that in (10).

Figure 11 describes the relationship between frequency ω and relative drift rate V_p of the MEMS inclinometer under the turntable test and the conical motion test. It can be seen that the V_p of the MEMS inclinometer in the turntable test is small, and the regularity of V_p changes with frequency are small. However, in the test of the conical motion, the V_p of the MEMS inclinometer in two axial directions shows an overall upward tendency according to the increasing frequency. Compared with the turntable testing method, the conical motion testing

method can induce drift problems in the MEMS inclinometer and is more suitable for the dynamic performance test of MEMS inclinometers.

4.2. Testing results for the attitude conical motion

The conical motion with 0.1° and 1° attitude deflection in the X-axis was selected to test the dynamic performance of the MEMS inclinometer. A comparison between the experimental results and the classical conical motion without attitude deflection is shown in Fig. 12. In these three groups of conical motion testing results under different conditions, the tilt sensitivities obtained by the MEMS inclinometer have the same trend. The differences between the two groups of attitude conical motion testing results and classical conical motion testing results are no more than 0.1 dB. Therefore, it is thought that the orthogonal compensation and gyroscopic drift compensation inside the MEMS inclinometer optimize the inclination angle output and weaken the influence of initial attitude deflection on the dynamic performance of the sensor.

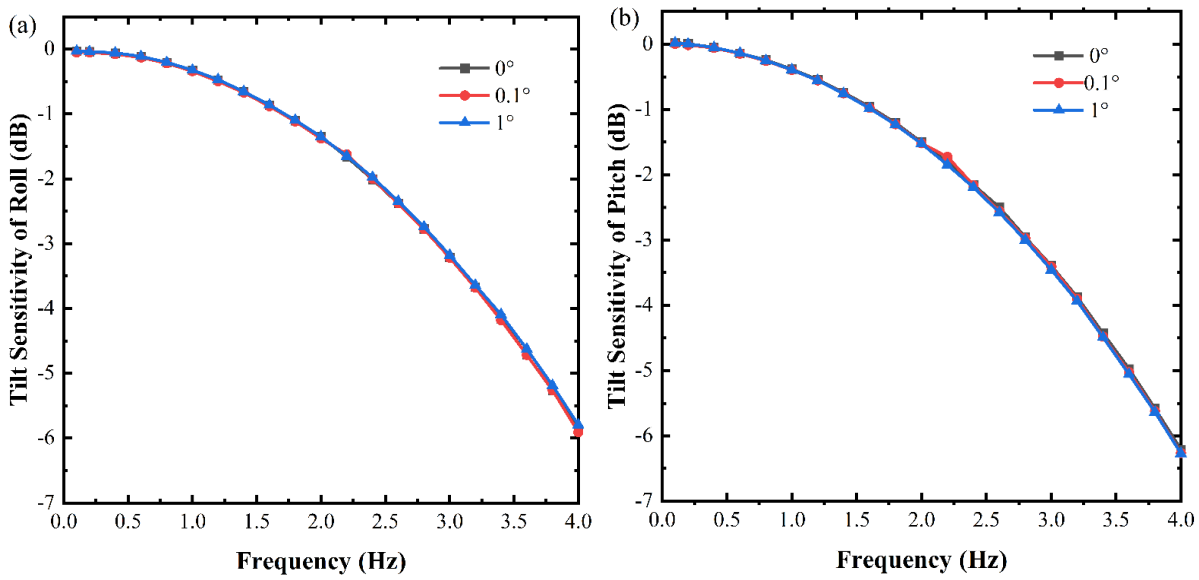

Fig. 12. Comparison of tilt amplitude sensitivities between the attitude conical motion test and the classical conical motion test: (a) tilt sensitivities of the roll axis; (b) tilt sensitivities of the pitch axis.

Equation (10) was used to calculate the relative drift rate V_p of the MEMS inclinometer in two groups of attitude conical motion tests. The results of the attitude conical motion and the classical conical motion were plotted together in Fig. 13. It can be seen that the V_p of the MEMS inclinometer of the attitude conical motion with the deflection of coordinate axis 0.1° is really close to that for the classical conical motion. The trend of the output inclination angle from the MEMS inclinometer in the roll-axis direction is obvious as the deflection increases to 1°. However, the V_p of the pitch-axis is small and stable. It is shown that the attitude conical motion with axial deflection has the advantage over the classical conical motion in exposing the mathematical drift of MEMS inclinometers in the corresponding axial direction.

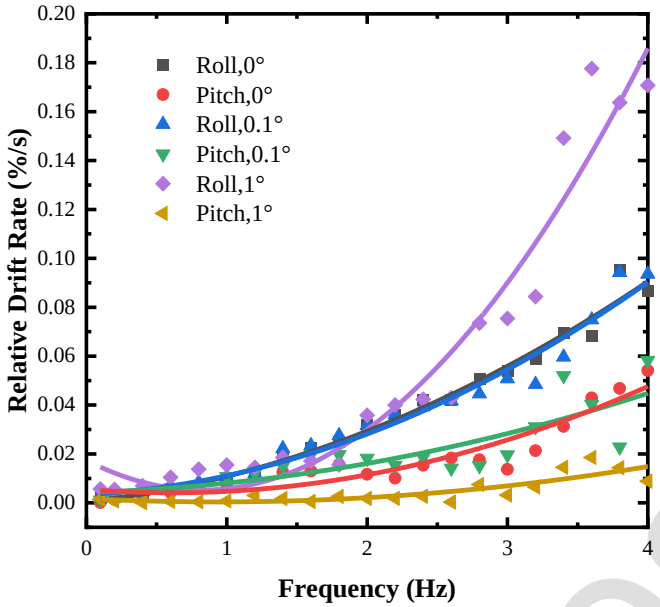

Fig. 13. Comparison of relative drift rates of the MEMS inclinometer in the attitude conical motion test and the classical conical motion test.

4.3. Testing results at the dual-frequency conical motion

To collect the inclination angle output of the roll-axis of the MEMS inclinometer, fixed angular vibration frequencies of 0.1 Hz, 0.5 Hz, 1 Hz, 1.5 Hz, and 2 Hz were successively set in the Y-axis, and changing angular vibration frequencies were selected upward in the X-axis. In Fig. 14, five groups of experimental data were drawn. It can be clearly seen that the curve tendency for each group of experimental results is synchronization, and the dynamic performance of the MEMS inclinometer decreases as the motion frequency increases. In the frequency range from 0.1 Hz to 0.4 Hz, the amplitude attenuation of the output inclination angle from the MEMS inclinometer is less than 0.1 dB. It can be considered that the MEMS inclinometer has a strong processing ability for its internal algorithm and outstanding visual appearance for its dynamic performance. When the motion frequency exceeds 0.4 Hz, the amplitude attenuation of the MEMS inclinometer increases. When the motion frequency reaches 4 Hz, the attenuation value exceeds 6 dB, and it is difficult to maintain stability of the dynamic performance.

The angular vibration frequency of the *Y*-axis was set at 1 Hz, and the angular vibration frequency of the *X*-axis was increased continuously. The relative drift rate V_p of the inclination angle output from the MEMS inclinometer under different dual-frequency conical motion conditions was calculated, and the results were compared with the results of the classical conical motion. As shown in Fig. 15, it is obvious that the increase in the V_p of the roll-axis by the MEMS inclinometer under the dual-frequency conical motion test is greater than that under the classical conical motion test. Although the motion frequency of the pitch-axis stays constant, the V_p of the pitch-axis of the MEMS inclinometer is affected by the change of the roll-axis motion frequency at low frequencies. The V_p of the pitch-axis tends to be stable as the roll-axis motion frequency increases over 3 Hz. It is shown that the dual-frequency conical motion not only has the advantage over the classical conical motion in exposing the mathematical drift of MEMS inclinometers in the corresponding axial direction but at low frequencies it also generates an influence on other moving axes.

Metrol. Meas. Syst., Vol. 30 (2023), No. 1
DOI: 10.24425/mms.2023.144398

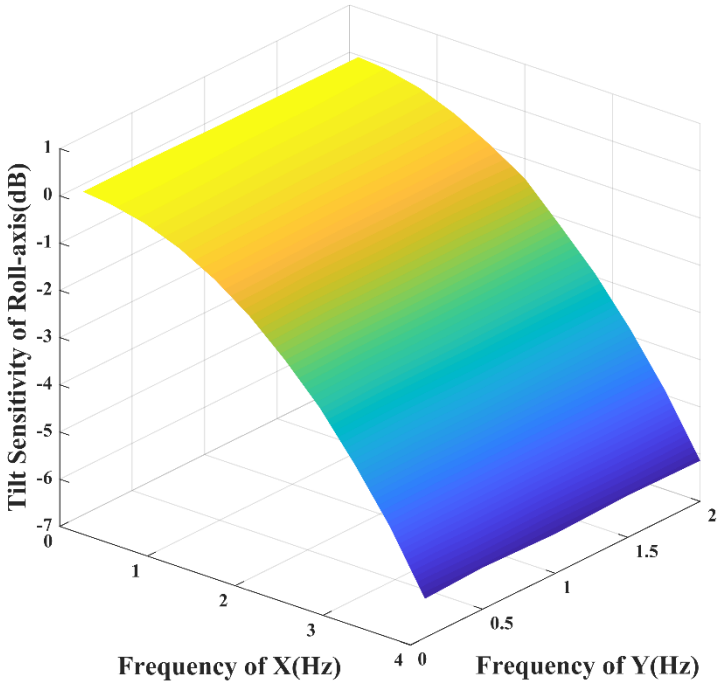

Fig. 14. Performance characteristic curve of the MEMS inclinometer in dual-frequency conical motion test.

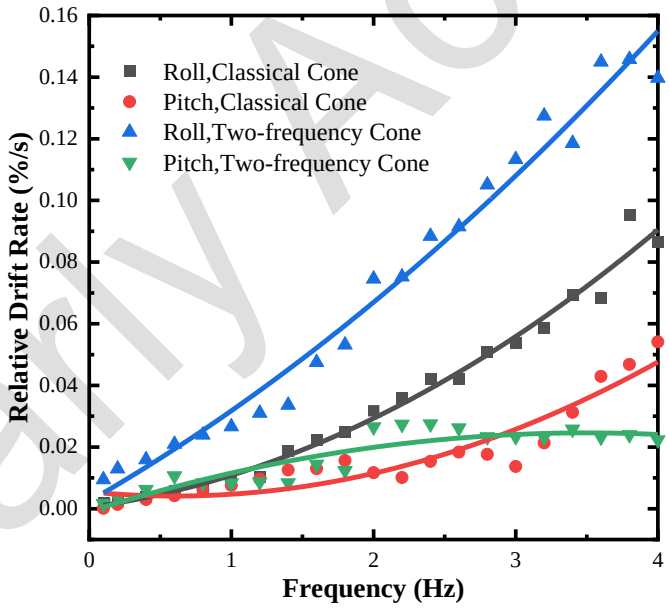

Fig. 15. Comparison of relative drift rates of the MEMS inclinometer in dual-frequency and classical conical motion tests.

5. Conclusions

Compared with uniaxial angular motions, the conical motion can provide inclination angle variation with two degrees of freedom with which it is easy to induce the exposure of drift and non-exchangeability of MEMS inclinometers. In addition to the classical conical motion, the other two conical motions take the influence of the initial attitude deflection and non-same frequency vibration factors into account, which makes the faulty working of the MEMS inclinometer embedded algorithm appear more often.

The conical motion has the ability to amplify the inclination drift tendency, and different conical motions cause different influences on the drift of MEMS inclinometers. The classical conical motion considers only the influence of motion frequency on MEMS inclinometers, and the experiment shows that the drift trend increases with the increase of motion frequency. When the frequency reaches 4 Hz, the relative drift rate is close to 0.1 %/s. The attitude conical motion takes the initial attitude angle deflection of the coordinate axis into consideration. When the attitude angle deflection gets to 1° and the frequency reaches 4 Hz, the relative drift rate approximates 0.2 %/s. When the attitude deflection increases to a certain value, the drift will obviously increase. The influence caused by different axial frequency changes on the drift is tested in the dual-frequency conical motion. When the motion frequency for the *X*-axis attains 4 Hz, the relative drift rate of the MEMS inclinometer roll-axis is close to 0.16 %/s, while the relative drift rate of the pitch-axis is reduced to 0.02 %/s. It can be found that when the motion frequency of an axial direction changes, both the inclination drift of its sensitive axial direction and the output of its orthogonal axial direction are influenced.

The dynamic tracking performance of the MEMS inclinometer is stable in the range of 0.1 Hz to 0.5 Hz, and the perception ability of the inclination angle is more than 98%. The perception ability of inclination angle continuously decreases as the motion frequency increases. When the motion frequency achieves 4 Hz, only a 50% inclination change can be detected. In the low frequency range, the optimization algorithm gives some compensation for the small change in initial attitude angle, and the deviation of output inclination angle data is less than 0.1 dB even if there is a 1° attitude angle deflection. Finally, the tested tilt sensitivity deviation of the MEMS inclinometer is less than 0.26 dB between the turntable and the conical motion, which verifies the validity of the proposed method.

Acknowledgements

This work was supported in part by National Natural Science Foundation of China (No. 52075512; No. 52265066; No. 62203132); National Key R&D Program of China (No. 2017YFF0205003); Doctor Foundation Project of Guizhou University (No. Guida Renji Hezhi [2020] 30); Youth Science and Technology Talents Development Project of Guizhou Education Department (No. Qianjiaohe KY [2022] 138).

References

[1] Shi, Q., Wang, H., He, T., & Lee, C. (2018, July). Self-powered triboelectric inertial sensor ball for IoT and wearable applications. In *Journal of Physics: Conference Series* (Vol. 1052, No. 1, p. 012030). IOP Publishing. https://doi.org/10.1088/1742-6596/1052/1/012030

[2] Setiawan, T., & Cysela, R. Y. (2021, October). Landslide Monitoring using Inclinometer with Micro Electromechanical System (MEMS). In *IOP Conference Series: Earth and Environmental Science* (Vol. 873, No. 1, p. 012024). IOP Publishing. https://doi.org/10.1088/1755-1315/873/1/012024

[3] Yang, M., Liu, Z., Cai, C., Wang, Y., Yang, J., & Yang, J. (2021). Monocular vision-based calibration method for the axial and transverse sensitivities of low-frequency tri-axial vibration sensors with the elliptical orbit excitation. *IEEE Transactions on Industrial Electronics*, *69*(12), 13763-13772. https://doi.org/10.1109/TIE.2021.3130325

[4] Gao, T., Sheng, W., Yin, Y., & Du, X. (2021, April). A Transfer Learning Based Unmanned Aerial Vehicle MEMS Inertial Sensors Fault Diagnosis Method. In *Journal of Physics: Conference Series* (Vol. 1852, No. 4, p. 042084). IOP Publishing. https://doi.org/10.1088/1742-6596/1852/4/042084

[5] Li, X., Xiao, W., & Fei, Y. (2015, September). Status quo and developing trend of MEMS-gyroscope technology. In *2015 Fifth International Conference on Instrumentation and Measurement, Computer, Communication and Control* (IMCCC) (pp. 727-730). IEEE. https://doi.org/10.1109/IMCCC.2015.159

[6] Liu, S., & Chen, G. (2021, March). Research on Noise Reduction Optimization of MEMS Gyroscope Based on Intelligent Technology. In *Journal of Physics: Conference Series* (Vol. 1802, No. 2, p. 022017). IOP Publishing. https://doi.org/10.1088/1742-6596/1802/2/022017

[7] Lu, J., Liu, X., & Zhang, H. (2018). Tilt measurement using inclinometer based on redundant configuration of MEMS accelerometers. *Measurement Science and Technology*, *29*(5), 055004. https://doi.org/10.1088/1361-6501/aaa504

[8] Balek, J., & Klokočník, P. (2021). Development of low-cost inclination sensor based on MEMS accelerometers. *IOP Conference Series: Earth and Environmental Science*, *906*(1), 012057. https://doi.org/10.1088/1755-1315/906/1/012057

[9] Łuczak, S. (2014). Dual-Axis Test Rig for Mems Tilt Sensors. *Metrology and Measurement Systems*, *21*(2), 351-362 https://doi.org/10.2478/mms-2014-0030

[10] Chan, L., Yuan, C., & Shi-feng, Z. (2015, May). A new multi-position calibration method for accelerometers of the inertial navigation system. In *The 27th Chinese Control and Decision Conference* (2015 CCDC) (pp. 6491-6494). IEEE. https://doi.org/10.1109/CCDC.2015.7161989

[11] Ye, L., Guo, Y., Dong, L., Yu, H., Nguyen, H., & Su, S. W. (2019). A fast-converge, real-time auto-calibration algorithm for triaxial accelerometer. *Measurement Science and Technology*, *30*(6), 065010. https://doi.org/10.1088/1361-6501/ab08c9

[12] Liu, H., Luo, W., & Lu, J. (2020). High precision fiber-optic gyroscope resolution test method based on low precision turntable. *IEEE Sensors Journal*, *20*(15), 8656-8662. https://doi.org/10.1109/JSEN.2020.2982982

[13] Yang, M., Liu, Z., Wang, Y., Cai, C., & Yang, J. (2022). Monocular vision-based multi-parameter dynamic calibration method used for the low-frequency linear and angular vibration sensors. *IEEE Transactions on Industrial Electronics*, *70*(5), 5365-5374. https://doi.org/10.1109/TIE.2022.3186310

[14] Chen, L., Zhou, Y., Zhang, D., Shu, X., & Liu, C. (2019) A dynamic angle metrology system based on fibre-optic gyroscope and rotary table. *Metrology and Measurement Systems*, *26*(3), 497–504. https://doi.org/10.24425/mms.2019.129574

[15] Xu, T., Xu, X., Bu, F., Xu, D., & Zhao, H. (2020). Three-position characterization for the adjustment of MEMS accelerometer scale factor. *Measurement Science and Technology*, *32*(3), 035020. https://doi.org/10.1088/1361-6501/abcbce

[16] Du, B., Shi, Z., Ding, M., Han, L., & Song, J. (2021). The calibration method for accelerometers in the redundant MEMS inertial navigation system. *Measurement Science and Technology*, *32*(9), 095004. https://doi.org/10.1088/1361-6501/abee52

[17] Särkkä, O., Nieminen, T., Suuriniemi, S., & Kettunen, L. (2017) A Multi-Position Calibration Method for Consumer-Grade Accelerometers, Gyroscopes, and Magnetometers to Field Conditions. *IEEE Sensors Journal*, *17*(11), 3470–3481. https://doi.org/10.1109/JSEN.2017.2694488

[18] Shang, Z., Ma, X., Li, M., & Liu, Y. (2015). A high-precision calibration method for MEMS gyroscopes. *International Journal of Precision Engineering & Manufacturing*, *16*(8), 1711–1716. https://doi.org/10.1007/s12541-015-0224-9

[19] Lu, J., Liang, S., & Yang, Y. (2017). A novel method of calibrating a MEMS inertial reference unit on a turntable under limited working conditions. *Measurement Science and Technology*, *28*(10), 105018. https://doi.org/10.1088/1361-6501/aa8219

[20] Lu, J., Liu, X., & Zhang, R. (2019). Calibration, Alignment, and Dynamic Tilt Maintenance Method Based on Vehicular Hybrid Measurement Unit. *IEEE Sensors Journal*, *19*(17), 7243–7253. https://doi.org/10.1109/JSEN.2019.2916067

[21] Jafari, M., Sahebjameyan, M., Moshiri, B., & Najafabadi, T. A. (2015). Skew redundant MEMS IMU calibration using a Kalman filter. *Measurement Science and Technology*, *26*(10), 105002. https://doi.org/10.1088/0957-0233/26/10/105002

[22] Lu, J., Yang, Y., Li, B., & Liu, M. (2017). Calibration of gyro G-sensitivity coefficients with FOG monitoring on precision centrifuge. *Measurement Science and Technology*, *28*(7), 075103. https://doi.org/10.1088/1361-6501/aa6c8b

[23] Wang, J., Deng, Z., Liang, X., & Liu, N. (2020). A MEMS gyroscope high-order calibration method for highly dynamic environments. *Measurement Science and Technology*, *32*(3), 035115. https://doi.org/10.1088/1361-6501/abca55

[24] Liu, Z., Cai, C., Yu, M., & Yang, M. (2017). Applying Spatial Orbit Motion to Accelerometer Sensitivity Measurement. *IEEE Sensors Journal*, *17*(14), 4483–4491. https://doi.org/10.1109/JSEN.2017.2703859

[25] Cheng, J., Liu, P., Wei, Z., & Luo, G. (2021). A novel MEMS-RIMU self-calibration method based on gravity vector observation. *Measurement Science and Technology*, *32*(5), 055108. https://doi.org/10.1088/1361-6501/abd798

[26] Liu, Z., Cai, C., Yang, M., & Zhang, Y. (2019). Testing of a MEMS Dynamic Inclinometer Using the Stewart Platform. *Sensors*, *19*(19), 4233. https://doi.org/10.3390/s19194233

[27] Wang, M., Wu, W., & He, X. (2018). Design and evaluation of high-order non-commutativity error compensation algorithm in dynamics. *2018 IEEE/ION Position, Location and Navigation Symposium (PLANS)*, 34–41. https://doi.org/10.1109/PLANS.2018.8373362

[28] Wang, M., Wu, W., Wang, J., & Pan, X. (2015). High-order attitude compensation in coning and rotation coexisting environment. *IEEE Transactions on Aerospace and Electronic Systems*, *51*(2), 1178–1190. https://doi.org/10.1109/TAES.2014.140084

[29] Zhang, S., Li, X., & Su, Z. (2016). Measuring and solving real coning motion of spinning carriers. *Proceedings of the Institution of Mechanical Engineers Part G Journal of Aerospace Engineering*, *230*(13), 2369–2378. https://doi.org/10.1177/0954410015624720

[30] Lee, T., & Kim, K. (2001). Analysis of the two-frequency coning motion with SDINS. *AIAA Guidance, Navigation, and Control Conference and Exhibit*. https://doi.org/10.2514/6.2001-4108

Qihang Yang received the B.Eng. degree from the Institute of Electrical Engineering of Shaoyang University, Shaoyang, China, in 2020. She is currently a postgraduate at the College of Measurement and Testing Engineering of Jiliang University, Hangzhou, China. Her research interests include vibration metrology and calibration.

Chenguang Cai received his Ph.D. degree in Precision Instrumentation and Mechanics from Beijing University of Aeronautics and Astronautics, Beijing, China, in 2007. From 2007 to 2009, he worked at the Nokia Research Center in Beijing, China as a post-doctoral research fellow. He was a visiting scientist at the Physikalisch-Technische Bundesanstalt, Braunschweig, Germany, in 2016. He is a member of the ISO TC 108/SC3 committee. He is currently a vice research fellow at the National Institute of Metrology, Beijing, China. His research interests include vibration calibration and optics measurement.

Ming Yang received the B.Eng. degree in Information Science and Technology in 2014, and the Ph.D. degree in Control Science and Engineering in 2020, both from Beijing University of Chemical Technology, Beijing, China. Currently, he is a lecturer at the Electrical Engineering College, Guizhou University, Guiyang, China. His main research interests include laser and machine vision detection, and vibration metrology and monitoring.

Ming Kong received the B.Eng. degree from the School of Instrument Science and Engineering of Southeast University, Nanjing, China, in 2000 and the Ph.D. degree in Measurement Technology and Instruments from the same university in 2005. He is currently working as a professor at Jiliang University. His research interests include multiphase flow detection, photoelectric detection technology, and development of measuring and detection equipment.

Metrol. Meas. Syst., Vol. 30 (2023), No. 1
DOI: 10.24425/mms.2023.144398

Zhihua Liu received the B.Eng. degree in Mechanical Engineering from Jilin University, Changchun, China, in 2010, and the Ph.D. degree in Mechanical Engineering from Tsinghua University, Beijing, China, in 2015. He is currently a vice research fellow at the National Institute of Metrology, China. His research interests include mechanisms and robotics as well methodology of mechanical testing.

Feng Liang received the B.Eng. degree in Mechanical Engineering from Jilin University, Changchun, China, in 2010. He is currently with the Shenyang Aircraft Corporation, Shenyang, China. His research interests include robotics machining and assembly.